

PAPER

# VUV photon emission from Ne clusters of varying sizes following photon and photoelectron excitations

To cite this article: Ltaief Ben Ltaief *et al* 2018 *J. Phys. B: At. Mol. Opt. Phys.* **51** 065002

View the [article online](#) for updates and enhancements.

## Related content

- [Determination of absolute cross sections for cluster-specific decays](#)  
Andreas Hans, André Knie, Marko Förstel et al.
- [Detecting ultrafast interatomic electronic processes in media by fluorescence](#)  
André Knie, Andreas Hans, Marko Förstel et al.
- [Fluorescence cascades after excitation of Xell 5p46p satellite states by synchrotron radiation](#)  
Christian Ozga, Philipp Reiß, Witoslaw Kielich et al.

# VUV photon emission from Ne clusters of varying sizes following photon and photoelectron excitations

Ltaief Ben Ltaief<sup>1</sup> , Andreas Hans<sup>1</sup>, Philipp Schmidt<sup>1</sup>, Xaver Holzapfel<sup>1</sup>, Florian Wiegandt<sup>2</sup>, Philipp Reiss<sup>1</sup>, Catmarna Küstner-Wetekam<sup>1</sup>, Till Jahnke<sup>2</sup>, Reinhard Dörner<sup>2</sup>, André Knie<sup>1</sup>  and Arno Ehresmann<sup>1</sup>

<sup>1</sup> Universität Kassel, Institut für Physik and Center for Interdisciplinary Nanostructure Science and Technology (CINSaT), Heinrich-Plett Straße 40, D-34132 Kassel, Germany

<sup>2</sup> Institut für Kernphysik, J. W. Goethe-Universität, Max-von-Laue-Str. 1, D-60438 Frankfurt am Main, Germany

E-mail: [ehresmann@physik.uni-kassel.de](mailto:ehresmann@physik.uni-kassel.de)

Received 23 November 2017, revised 16 January 2018

Accepted for publication 31 January 2018

Published 21 February 2018



CrossMark

## Abstract

Vacuum ultraviolet (VUV) fluorescence emission from neon clusters of different sizes is investigated after excitation with photons of energies between 34 and 49 eV, i.e. near and far below the Ne 2s-electron photoionization threshold. Undispersed VUV fluorescence (<120 nm) excitation functions in the Ne 2s-regime display a series of distinct features attributed to 2s → np resonant cluster excitations with subsequent cluster-specific decays. Features connected with resonant interatomic Coulombic decay are visible for all cluster sizes. For larger clusters they appear to be less prominent due to additional emissions. This emission has a threshold energy of 35.8 eV and increases with exciting-photon energy. It also increases with increasing cluster size and is interpreted as being caused by inelastically scattered 2p-photoelectrons (photoelectron impact induced luminescence).

Keywords: electronic excitation and relaxation process, resonant interatomic Coulombic decay, Ne clusters, inelastic intracluster photoelectron scattering, VUV fluorescence

(Some figures may appear in colour only in the online journal)

## 1. Introduction

The interaction between high-energy photons and weakly bound systems such as van-der-Waals or hydrogen-bonded clusters usually causes ionization. Parallel to or as a consequence of a photoelectron ejection event there are mechanisms leading to a variety of electronic excitation processes where a larger amount of energy is deposited in the electronic system of the cluster. This energy may be released by intra-atomic processes like Auger electron or fluorescence emission, or by interatomic relaxation processes involving neighboring sites, like the well-known ultrafast and efficient non-radiative interatomic/intermolecular Coulombic decay (ICD) [1] which is in the focus of numerous theoretical and experimental investigations [2–12]. In the latter case the

excess energy of an inner-valence ionized atom or molecule is transferred to a neighboring site to eject slow electrons (ICD electrons), thereby ionizing this entity. Electrons with low kinetic energy are generally proven to be genotoxic and can efficiently induce irreparable damage in living tissue [13, 14]. In extended weakly bound systems, however, additional slow secondary electrons can be produced by inelastic scattering of fast photoelectrons or Auger-electrons [15] and may experimentally mask the ICD electrons. These two effects have been investigated in the past [16, 17] on Ne clusters. Additionally it was found that the probability for inelastic scattering increases with cluster size. Inelastic intracluster photoelectron scattering was investigated before by photoemission methods, and it was shown to lead to the production of excitonic satellites that are not present in the atomic case [18, 19], and

also to the formation of zero-kinetic-energy photoelectrons [20]. Additionally intracluster inelastic scattering of emitted ICD electrons may occur [21] as shown for Ne clusters multiply excited by intense free electron laser radiation, and it was found that it affects the ICD relaxation of Ne bulk atoms.

As reported in previous work [22–24] vacuum ultraviolet (VUV) and UV/visible fluorescence emissions can be used to efficiently track a special variety of ICD, the resonant ICD (RICD) process [25–31]. Due to the longer escape length of photons versus slow electrons in dense matter this method may potentially be used to investigate RICD in real samples. Furthermore, fluorescence spectroscopy can be used to study cluster size effects on a variety of processes occurring in extended systems [32–34]. Here we report a systematic experiment of VUV fluorescence emission from large Ne clusters of varying size after being excited by photons of energies near and far below the Ne 2s-electron photoionization threshold.

## 2. Experimental methods

The experiment was performed with an established set-up for photon-induced fluorescence spectroscopy [35] at the synchrotron radiation (SR) facility SOLEIL, Paris, at the PLEIADES beamline in its multi-bunch operation mode. A slit width of 300  $\mu\text{m}$  of the plane grating monochromator was chosen corresponding to a bandwidth of the exciting photons of about 13 meV at 44 eV. The Ne cluster jet was produced by supersonic expansion through a 32  $\mu\text{m}$  diameter nozzle cooled by a liquid helium flow cryostat which separates the high pressure stagnation chamber from the vacuum in the expansion chamber.

Ne clusters covering the average size range from  $\langle N \rangle \sim 40$  up to  $\langle N \rangle \sim 7000$  were used in the experiment. The average cluster size was varied by choosing appropriate expansion parameters with the temperature fixed at 60 K and stagnation pressure ranging from 3 up to 11 bar; except for the average cluster size of  $\langle N \rangle \sim 7000$  with 40 K and 9 bar. The average cluster sizes were estimated according to [36]. After passing through a 1.5 mm diameter skimmer, the jet entered the interaction chamber, where it crossed the linearly polarized photon beam of the monochromatized SR.

A stack of two bare microchannel plates (MCPs) was mounted in a differentially pumped chamber, separated from the interaction chamber by an aperture and used to detect undispersed VUV photons. As the quantum efficiency for photons drops below 1% for photon wavelengths longer than about 120 nm (see, e.g. [37, 38]) and remains at around 10% for shorter wavelengths this detector will essentially detect photons with wavelengths below 120 nm. An operating voltage of  $-2580$  V was applied to the front of the MCPs stack with respect to the rear side of the second MCP. By that, electrons were rejected. Additionally, a  $-133$  V voltage was applied between the rear side of the second MCP and the anode, which was kept at ground potential. Positively-charged ions were rejected by a mesh in front of the first MCP set to  $+36$  V. A  $-19.3$  V voltage was applied to an electrically

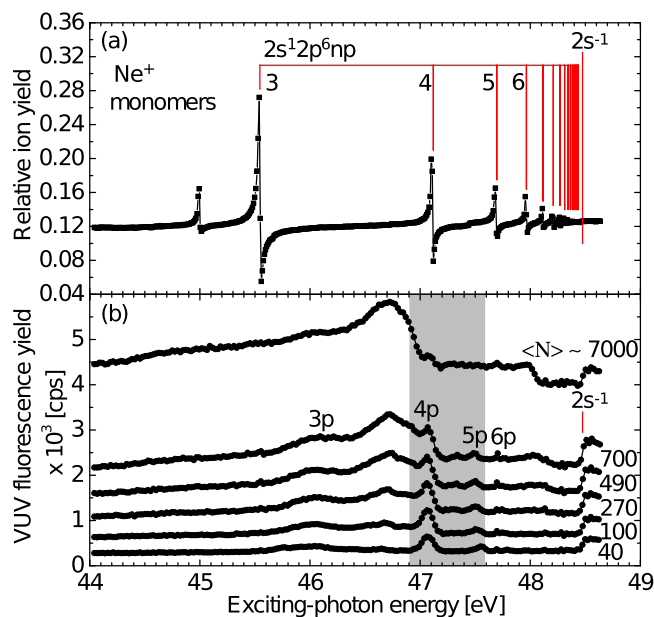


**Figure 1.** (a) Relative  $\text{Ne}^+$ -ion yields of free Ne atoms normalized on the photocurrent of the last refocusing mirror. (b) VUV fluorescence excitation functions below the Ne 2s-electron photoionization threshold for different average sizes of Ne clusters. The grey-shaded region from 46.9 to 47.6 eV highlights the two RICD features at about 47.06 and 47.51 eV [22]. The assignments have been made according to [39] for atomic  $2s \rightarrow np$  excitations energies in (a), and [43] for the  $2s \rightarrow np$  ( $n = 3, 4, 5, 6$ ) cluster excitations in (b). The Ne 2s-electron photoionization threshold is pointed out by a vertical solid line at 48.475 eV [19, 39] in (a) and (b).

connected electrode opposite to the detector aperture in order to measure the yield of positively-charged  $\text{Ne}^+$ -ions. A Faraday cup mounted behind the interaction region was used for monitoring the transmitted light through the cluster jet.

First, the  $\text{Ne}^+$ -ion yield from an atomic Ne jet was recorded in an exciting-photon energy range of 44.0–48.7 eV with energy steps of 10 meV and then normalized for the photocurrent of the last refocusing mirror. Undispersed VUV fluorescence yield was collected in the exciting-photon energy range of 44.0–48.7 eV with energy steps of 25 meV, and in the range of 34.0–48.7 eV with energy steps of 100 meV for different cluster sizes. Except for very big clusters ( $\langle N \rangle \sim 7000$ ), here the undispersed VUV fluorescence yield was recorded with an energy step width of 250 meV in the exciting-photon energy range of 34.0–49.0 eV. The exciting-photon energy was calibrated against the 2s-ionization threshold of Ne atoms at 48.475 eV [19, 39], which is present in the recorded fluorescence excitation spectra due to the interaction of the SR with the monomers in the produced mixed monomer/cluster beam.

## 3. Results and discussion

Figure 1(a) shows the relative yield of  $\text{Ne}^+$ -ions after photoionization of Ne atoms for exciting-photon energies between 44.0 and 48.7 eV, normalized for the flux of the exciting photons. The  $\text{Ne}^+$ -ion yield is dominated by a series

of Fano-profiles [39–41] corresponding to autoionizing  $2s^1 2p^6 np$ -Rydberg states embedded in the  $2p$ -electron continuum. This Rydberg series converges to the Ne  $2s$ -electron ionization threshold at 48.475 eV [19, 39]. In addition, the atomic Ne<sup>+</sup>-ion yield exhibits a feature at around 44.98 eV due to a transition to the atomic  $2p^4(^3P)3s(^2P_{1/2,3/2})3p$ -state and its subsequent autoionization [39]. These well-known features measured on a pure atomic jet (no clusters in the jet) have been used to calibrate the scale of the exciting-photon energy and to check the linearity of the nominal versus the true photon-energy scale of the beamline.

Figure 1(b) displays the undispersed VUV fluorescence excitation functions recorded by the MCP detector for Ne clusters of several average cluster sizes (from 40 atoms up to 7000 atoms per cluster). This graph is used for the discussion of the spectral features and is not yet normalized for the exciting-photon-flux.

The recorded total VUV fluorescence excitation functions of the mixed Ne-atom/cluster jet exhibits for all cluster sizes a sudden increase at an exciting-photon energy of 48.475 eV. This increase is due to the  $2s$ -electron photoionization in Ne atoms and the subsequent fluorescence transitions  $2s^1 2p^6 \ ^2S_{1/2} \rightarrow 2s^2 2p^5 \ ^2P_{3/2,1/2}$  at 46.0 and 46.2 nm within Ne II [42].

In the present experiment the following observations are made which display characteristic changes with increasing cluster size: (1) at lower energies within the investigated exciting-photon energy range the fluorescence intensity is structureless and continuously increases for beam conditions producing larger average cluster sizes. (2) The fluorescence signal recorded for the smallest cluster size shows a series of features, which may be identified as  $2s \rightarrow np$  excitations of cluster-surface atoms [43] resulting in VUV fluorescence emission. These features are visible for all cluster sizes but appear to be less prominent in the fluorescence excitation functions of the larger clusters due to increasing fluorescence intensity around the features. The grey-shaded exciting-photon energy region of figure 1(b) highlights the two fluorescence features at 47.06 and 47.51 eV which were interpreted in previous works as originating from RICD [22]. (3) A number of additional comparatively broad features are becoming more prominent as the average cluster size increases. The most obvious example is the feature centered at around 46.66 eV.

We discuss in the following the three observations:

- (1) The structurelessly increasing intensity at small exciting-photon energies is interpreted as due to fluorescence excitation by inelastically scattered  $2p$ -photoelectrons (photoelectron impact induced fluorescence). The process leading to VUV fluorescence emission after photoelectron impact is exciton excitation in the cluster. Formation of excited ions with VUV fluorescence emission is not possible for the present exciting-photon energies. In order to experimentally investigate this hypothesis the exciting-photon energy range has been widened as compared to the experiments of figure 1: figure 2 shows the VUV fluorescence excitation

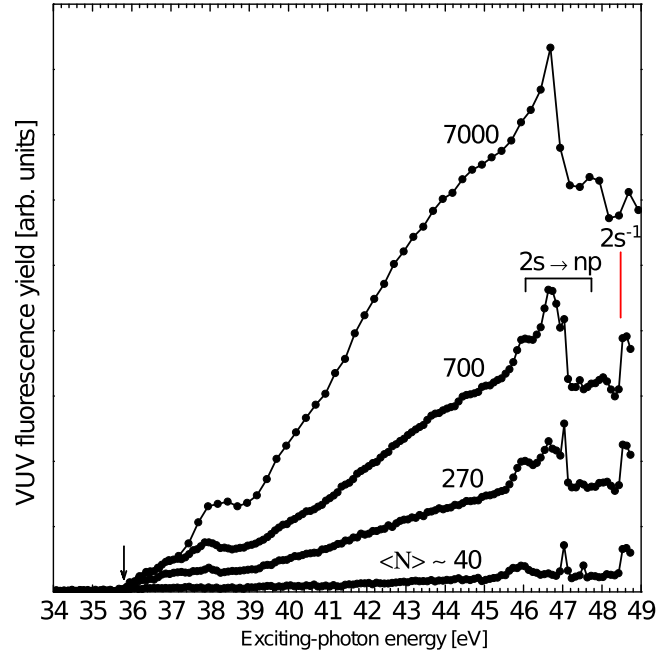


**Figure 2.** VUV fluorescence excitation functions for four average cluster sizes ( $\langle N \rangle \sim 40, 270, 700$  and  $7000$ ) of Ne clusters in the exciting-photon energy range of 34.0–49.0 eV, after being first background-corrected and then normalized for the flux of the exciting photons. The prominent features in the exciting-photon energy range of 45.0–47.8 eV correspond to the  $2s \rightarrow np$  resonant excitations [43] in Ne clusters. The structureless increase of the fluorescence signal observed at lower exciting-photon energies and above the exciton excitation is interpreted as due to fluorescence excitation by inelastically scattered  $2p$ -photoelectrons, as discussed in the text. The onset of the measured VUV fluorescence signals of clusters and the Ne  $2s$ -electron photoionization threshold are indicated by a vertical arrow at about 35.8 eV and by a vertical solid line at 48.475 eV [19, 39], respectively.

functions of Ne clusters for exciting-photon energies from 34.0 eV up to 49.0 eV and for four selected average cluster sizes ( $\langle N \rangle \sim 40, 270, 700$  and  $7000$ ).

The onset of the almost continuous fluorescence signal increase lies at  $\approx 35.8$  eV. In the data displayed in figure 2, the constant background of the detector due to electronic noise and a small contribution of stray light from incident synchrotron beam has been determined at exciting-photon energies below 35.5 eV and assumed to be constant throughout the whole exciting-photon energy range. This background has then been subtracted from the raw data. Then the background-corrected data has been normalized to the current of the last refocusing mirror in the beamline, as a measure for the incoming photon-flux. Care has been taken that beam position variations during data acquisition did not influence the proportionality between measured mirror current and photon-flux in the interaction region by comparing the mirror current to the signal measured by the Faraday cup mounted behind the interaction region.

Closely above the onset energy a broad feature at  $\approx 37.9$  eV is seen, which becomes more and more prominent with increasing cluster size. It is attributed to

photoelectron impact excitation of the lowest excitonic state in the cluster as identified in [18]. The required electron energy to excite this state is about 17.6 eV [18, 44], which together with the 2p-electron binding energy in solid Ne (20.3 eV [45]) corresponds to 37.9 eV, in good agreement with the observation. At exciting-photon energies above the photoelectron impact excitation the observed fluorescence signal increases approximately linearly with energy with a larger increase for gas jet conditions resulting in larger clusters. If this signal is due to inelastically scattered 2p-photoelectrons, the cross section of the VUV fluorescence emission  $\sigma_{fl}(h\nu)$  seen by the detector must be proportional to the product of the cross sections of 2p-electron photoionization  $\sigma_{2p}(h\nu)$  and for VUV fluorescence emission by electron impact  $\sigma_{fl,EI}(E_{kin}) = \sigma_{fl,EI}(h\nu - E_{B,2p})$ :

$$\sigma_{fl}(h\nu) \propto \sigma_{2p}(h\nu) \cdot \sigma_{fl,EI}(h\nu - E_{B,2p}).$$

Here  $h\nu$  is the exciting-photon energy,  $E_{kin}$  is the kinetic energy of the photoelectron, and  $E_{B,2p}$  is the binding energy of the Ne 2p-electron in solid Ne (20.3 eV [45]). The measured VUV emission onset energy of  $\approx 35.8$  eV is smaller than the sum of  $E_{B,2p}$  and the threshold energy for electron induced VUV fluorescence excitation in Ne atoms (16.683 eV [46, 47], corresponding to the decay of the  $2p^5 \ ^2P_{3/2} \ 3s \ [3/2]$  level to the Ne ground state). Spectrally resolved VUV fluorescence of solid Ne after 2.5 keV electron impact, however, revealed a smooth onset of fluorescence between 15 and 16 eV of emitted-photon energy [48]. The corresponding fluorescence feature has been attributed to molecular type self-trapped excitons. In the spectrum of this work a huge peak with finer structure at around 16.7 eV is visible, which has been attributed to atomic-type self-trapped excitons. As we could not find measured VUV fluorescence excitation functions of solid Ne in literature the cited work can only be used for identifying possible spectral features but not for an analysis of corresponding cross sections for the relevant processes. We conclude that these excitonic features can well be excited by 2p-photoelectrons in our experiment and that observed VUV fluorescence emission close to the fluorescence onset energy in the present experiment is due to clusters (excitonic excitations) only.

The 2p-electron photoionization cross section does not vary significantly in the exciting-photon energy range between 34 and 49.0 eV, when resonances are neglected for the moment [49]. It is therefore assumed to be constant. The electron impact induced VUV fluorescence excitation function of Ne atoms, however, has a steep, almost linear increase with electron energy in the energy range between fluorescence onset and about 15 eV above [50]. If we assume a similar dependence of fluorescence excitation on the electron energy for the clusters, also the product of these two cross sections will increase almost linearly with

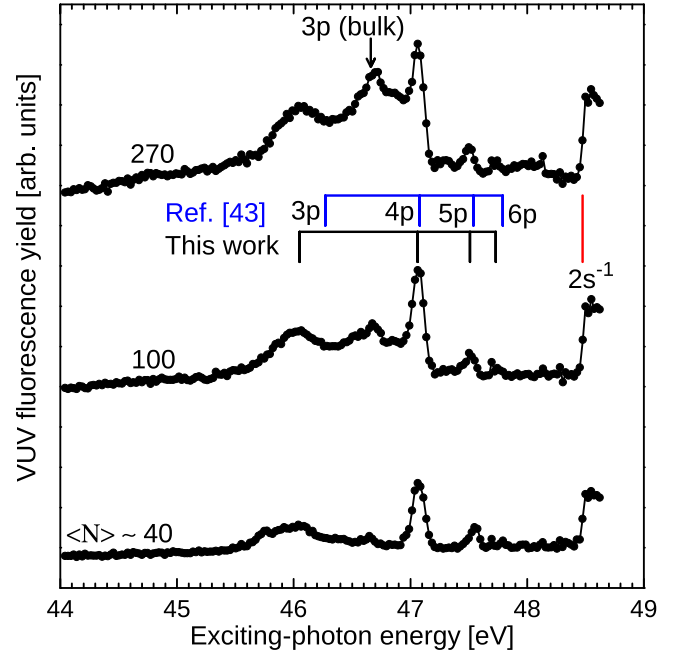


**Figure 3.** VUV fluorescence excitation functions below the Ne 2s-electron photoionization threshold for  $\langle N \rangle \sim 40, 100$  and  $270$  as average sizes of Ne clusters. The vertical solid lines in blue and black indicate the energies of the  $2s \rightarrow np$  excitations in Ne clusters obtained in [43] for  $\langle N \rangle = 140$  and in this work for  $\langle N \rangle \sim 100$ , respectively. The vertical arrow points out the observed cluster bulk excitation at about 46.66 eV. The Ne 2s-electron photoionization threshold is marked by a vertical solid line at 48.475 eV [19, 39]. The narrow features in the VUV fluorescence signal for  $\langle N \rangle \sim 40$  and close to the Ne 2s-electron photoionization threshold are the resonant excitations of the Ne I  $2s^1 2p^6 np$ -Rydberg states with subsequent fluorescence decay in the free Ne atoms [51].

exciting-photon energy. Additionally, as the kinetic energy of the emitted electron is increasing, more channels for VUV fluorescence emission will open.

Consequently, the presented evidences suggest that the fluorescence intensity increase indicates an intracluster photoelectron-impact induced fluorescence excitation, which gets more and more significant with increasing cluster size. Regardless of the energy transfer process that leads to the occurrence of ICD in a cluster, in the present experiment self-absorption may also appear in Ne clusters when a photon is firstly emitted by an excited atom and then absorbed by a neighboring atom. This effect, however, cannot be quantified in the present experiment.

- (2) Figure 3 shows separately the VUV fluorescence excitation functions observed for the smallest average cluster sizes ( $\langle N \rangle \sim 40, 100, 270$ ), and which are already presented above in figure 1(b) of the present experiment. As for such experimental conditions photoelectron-impact induced fluorescence is still weak, narrow features belonging to resonant excitations of Ne I  $2s^1 2p^6 np$ -Rydberg states with high principal quantum number  $n$  of uncondensed Ne atoms are clearly seen close to the Ne 2s-electron photoionization threshold in the recorded fluorescence excitation function for  $\langle N \rangle \sim 40$ . The former atomic

**Table 1.** Experimental  $2s \rightarrow np$  cluster transition energies in comparison with the observation in [43] for  $\langle N \rangle = 140$ . The cluster transition energies refer to the VUV fluorescence yield of Ne cluster for  $\langle N \rangle \sim 100$  and are obtained by fitting each resonant cluster feature with a Gaussian function. The numbers in parentheses indicate the  $1\sigma$  uncertainties for the experimental energy values.

Transitions	$E_{\text{exp}}$ (eV)	$E_{\text{Ref.}}$ [43] (eV)
$2s \rightarrow 3p$	46.05(3)	46.27
$2s \rightarrow 4p$	47.06(3)	47.08
$2s \rightarrow 5p$	47.51(3)	47.54
$2s \rightarrow 6p$	47.73(5)	47.79

fluorescence features are already observed before by other authors [51] in case of pure Ne gas. Apart from these atomic fluorescence features and their subsequent fluorescence decays, other features in the fluorescence excitation function for  $\langle N \rangle \sim 40$  as well for  $\langle N \rangle \sim 100$  and 270 are belonging to resonant cluster excitations. A comparison between VUV fluorescence excitation functions measured for a pure atomic Ne jet and a cluster beam produced with an average cluster size of  $\langle N \rangle \sim 20$  have been already reported in previous works [22, 23]. The exciting-photon energies of peaks in the cluster fluorescence excitation functions agree with energies calculated and measured for  $2s \rightarrow np$  ( $n > 2$ ) cluster excitations resulting in ion production [43], except for the energy of the  $2s \rightarrow 3p$  cluster excitation which is observed in our case shifted to lower energy by about 0.22 eV compared to the observation in [43] for  $\langle N \rangle = 140$ , as indicated in figure 3.

Table 1 compares the energy positions of the  $2s \rightarrow np$  cluster transitions obtained by using a Gaussian fit with the finding in [43]. Compared to the atomic Ne  $2s \rightarrow np$  Rydberg resonances shown in figure 1(a), the  $2s \rightarrow np$  ( $n > 3$ ) cluster excitations are relatively shifted to lower energies whereas the  $2s \rightarrow 3p$  cluster excitation undergoes a clear energy shift towards higher energy by about 0.51 eV.

Essentially no shifts of the exciting-photon energies of the observed peaks with changing cluster size are seen within the resolution of the current experiment. Whereas the 4p, 5p, and 6p excitations appear as well defined peaks (apart from the 6p excitation which is observed weakly for  $\langle N \rangle \sim 40$ ) in the fluorescence excitation functions, the feature around the energy of the 3p excitation is rather broad. With increasing cluster size ( $\langle N \rangle > 40$ ) the features at the 4p, 5p, and 6p excitations are less and less prominent due to an increasing contribution of photoelectron-impact induced fluorescence. Observed features in the fluorescence excitation functions of the smallest clusters do agree in energies with the corresponding features in previous work [22–24].

- (3) The observed feature at  $\approx 46.66$  eV increases in intensity relative to the  $2s \rightarrow np$  excitation peaks with increasing average cluster size. It appears weak for clusters smaller than  $\langle N \rangle < 100$  and becomes more and more prominent when the cluster becomes larger than  $\langle N \rangle \sim 100$ . In clusters the ratio of the number of bulk

atoms to surface atoms increases with increasing cluster size. This feature can therefore be assigned to a bulk transition, as highlighted by an arrow in figure 3. The exciting-photon energy ( $\approx 46.66$  eV) at which this feature emerges can be compared with features in published works observed in the total electron [52, 53] and ion desorption [52] yields from condensed Ne. There the bulk component of the  $2s \rightarrow 3p$  excitation is observed at 46.9 eV and 46.85 eV, respectively. Although these exciting-photon energies are 0.24 eV and 0.19 eV higher than the one we measure, we tentatively identify the observed feature at  $\approx 46.66$  eV with the  $2s \rightarrow 3p$  excitation of the bulk. Note that in [4] the same identification is also used for the observed bulk feature in Ne clusters for  $\langle N \rangle = 70$ , observed there at 47.5 eV. An energy shift of this feature with increasing cluster size cannot be determined from the current experimental data but this feature becomes significantly broader with increasing cluster size; especially for  $\langle N \rangle \sim 7000$  (see figure 1(b)) where the shape of the VUV fluorescence excitation function is comparable with the previously obtained absorption cross section of solid Ne [54].

## 4. Conclusion

We have reported VUV fluorescence emission from variable size Ne clusters triggered by photoelectron impact and also by ultrafast electronic relaxation processes, specifically the RICD, after SR excitation. At exciting-photon energies near the Ne  $2s$ -electron photoionization threshold, the cluster size dependent VUV fluorescence excitation functions show a series of distinct cluster fluorescence features; four of which are attributed to the resonant  $2s \rightarrow np$  ( $n = 3, 4, 5, 6$ ) excitations of atoms on the cluster surface and one to excitation of atoms in the bulk. Included in these are the ones previously identified to emerge from RICD. At lower exciting-photon energies, a structureless VUV fluorescence is observed increasing with exciting-photon energy as well with cluster size. It is interpreted as due to inelastic scattering of the initially outgoing  $2p$ -photoelectrons with condensed neutral Ne atoms.

## Acknowledgments

This work was supported by the Hesse State Initiative for the Development of Scientific and Economic Excellence (LOEWE) in the LOEWE-Focus Electron Dynamics of Chiral Systems (ELCH) and by a BMBF grant under promotion code number 05K13RK1. We thank SOLEIL for beamtime allocation, the SOLEIL staff for support, and the PLEIADES team for assistance and discussions during the beamtime, particularly Catalin Miron and John Bozek. Funding by the Deutsche Forschungsgemeinschaft via the Forschergruppe

1789 and Deutscher Akademischer Austauschdienst (DAAD) is gratefully acknowledged.

## ORCID iDs

Ltaief Ben Ltaief  <https://orcid.org/0000-0002-2492-895X>

André Knie  <https://orcid.org/0000-0002-2208-8838>

## References

- [1] Cederbaum L S, Zobeley J and Tarantelli F 1997 *Phys. Rev. Lett.* **79** 4778
- [2] Santra R, Zobeley J and Cederbaum L S 2001 *Phys. Rev.* **64** 245104
- [3] Averbukh V et al 2011 *J. Electron Spectrosc. Relat. Phenom.* **183** 36–47
- [4] Marburger S, Kugeler O, Hergenhahn U and Möller T 2003 *Phys. Rev. Lett.* **90** 203401
- [5] Jahnke T et al 2004 *Phys. Rev. Lett.* **93** 163401
- [6] Öhrwall G et al 2004 *Phys. Rev. Lett.* **93** 173401
- [7] Kuleff A I and Cederbaum L S 2007 *Phys. Rev. Lett.* **98** 083201
- [8] Jahnke T et al 2007 *J. Phys. B: At. Mol. Opt. Phys.* **40** 2597–606
- [9] Hergenhahn U 2011 *J. Electron Spectrosc. Relat. Phenom.* **184** 78
- [10] Schnorr K et al 2013 *Phys. Rev. Lett.* **111** 093402
- [11] Förstel M, Arion T and Hergenhahn U 2013 *J. Electron Spectrosc. Relat. Phenom.* **191** 16–9
- [12] Jahnke T 2015 *J. Phys. B: At. Mol. Opt. Phys.* **48** 082001
- [13] Boudaïffa B, Cloutier P, Hunting D, Huels M A and Sanche L 2000 *Science* **287** 1658–60
- [14] Alizadeh E, Orlando T M and Sanche L 2015 *Annu. Rev. Phys. Chem.* **66** 379–98
- [15] Pimblott S M and LaVerne J A 2007 *Radiat. Phys. Chem.* **76** 1244–7
- [16] Mücke M, Arion T, Förstel M, T Lischke T and Hergenhahn U 2015 *J. Electron Spectrosc. Relat. Phenom.* **200** 232–8
- [17] Barth S, Marburger S, Kugeler O, Ulrich V, Joshi S, Bradshaw A M and Hergenhahn U 2006 *Chem. Phys.* **329** 246–50
- [18] Hergenhahn U, Kolmakov A, Riedler A M, De Castro A R B, Löffken O and Möller T 2002 *Chem. Phys. Lett.* **351** 235–41
- [19] Joshi S, Barth S, Marburger S, Ulrich V and Hergenhahn U 2006 *Phys. Rev.* **73** 235404
- [20] Knop A, Jochims H W, Kilcoyne A L D, Hitchcock A P and Rühl E 1994 *Chem. Phys. Lett.* **223** 553–60
- [21] Iablonskyi D et al 2016 *Phys. Rev. Lett.* **117** 276806
- [22] Knie A et al 2014 *New J. Phys.* **16** 102002
- [23] Hans A, Knie A, Förstel M, Schmidt P, Reiß P, Ozga C, Hergenhahn U and Ehresmann A 2016 *J. Phys. B: At. Mol. Opt. Phys.* **49** 105101
- [24] Hans A et al 2017 *Chem. Phys.* **482** 165–8
- [25] Barth S, Joshi S, Marburger S, Ulrich V, Lindblad A, Öhrwall G, Björneholm O and Hergenhahn U 2005 *J. Chem. Phys.* **122** 241102
- [26] Aoto T, Ito K, Hikosaka Y, Shigemasa E, Penent F and Lablanquie P 2006 *Phys. Rev. Lett.* **97** 243401
- [27] Trinter F et al 2013 *Phys. Rev. Lett.* **111** 233004
- [28] O’Keeffe P et al 2013 *J. Phys. Chem. Lett.* **4** 1797–801
- [29] Gokhberg K, Averbukh V and Cederbaum L S 2006 *J. Chem. Phys.* **124** 144315
- [30] Kopelke S, Gokhberg K, Cederbaum L S and Averbukh V 2009 *J. Chem. Phys.* **130** 144103
- [31] Jabbari G, Klaiman S, Chiang Y-C, Trinter F, Jahnke T and Gokhberg K 2014 *J. Chem. Phys.* **140** 224305
- [32] Karnbach R, Joppien M, Stapelfeldt J, Wörmer J and Möller T 1993 *Rev. Sci. Instrum.* **64** 2838–49
- [33] Rühl E, Heinzl C and Jochims H W 1993 *Chem. Phys. Lett.* **211** 403–9
- [34] Björneholm O, Federmann F, Joppien M, Fössing F, Kakar S, Von. Pietrowski R and Möller T 1996 *Surf. Rev. Lett.* **3** 299–306
- [35] Schmoranzler H, Liebel H, Vollweiler F, Müller-Albrecht R, Ehresmann A, Schartner K-H and Zimmermann B 2001 *Nucl. Instrum. Methods Phys. Res. A* **467–468** 1526–8
- [36] Buck U and Krohne R 1996 *J. Chem. Phys.* **105** 5408–15
- [37] Martin C and Bowyer S 1982 *Appl. Opt.* **21** 4206–7
- [38] Hamamatsu Photonics K K 2006 *MCP Assembly* (Iwata City: Electron Tube Division 314–5, Shimokanzo, Iwata City, Shizuoka Pref., 438-0193, Japan)
- [39] Schulz K, Domke M, Püttner R, Gutiérrez A, Kaindl G, Miecznik G and Greene C H 1996 *Phys. Rev. A* **54** 3095–112
- [40] Fano U 1961 *Phys. Rev.* **124** 1866–78
- [41] Fano U and Cooper J W 1965 *Phys. Rev.* **137** 1364–A
- [42] Schartner K-H, Möbus B, Mentzel G, Ehresmann A, Vollweiler F and Schmoranzler H 1992 *Phys. Lett. A* **169** 393–5
- [43] Flesch R, Kosugi N, Knop-Gericke A and Rühl E 2014 *Z. Phys. Chem.* **228** 387–403
- [44] Schwentner N, Koch E E and Jortner J 1985 *Springer Tracts in Modern Physics* vol 107 (Heidelberg: Springer)
- [45] Schwentner N, Himpfel F-J, Saile V, Skibowski M, Steinmann W and Koch E E 1975 *Phys. Rev. Lett.* **34** 528–31
- [46] Brunt J N H, King G C and Read F H 1977 *J. Phys. B: At. Mol. Phys.* **10** 3781
- [47] Zeman V, Bartschat K, Norén C and McConkey J W 1998 *Phys. Rev. A* **58** 1275
- [48] Coletti F, Debever J M and Zimmerer G 1985 *J. Chem. Phys.* **83** 49
- [49] Becker U and Shirley D 1996 *VUV and Soft X-Ray Photoionization* (New York: Plenum Press) pp 135–77
- [50] Kanik I, Ajello J M and James G M 1996 *J. Phys. B: At. Mol. Opt. Phys.* **29** 2355–66
- [51] Lablanquie P et al 2000 *Phys. Rev. Lett.* **84** 431–4
- [52] Wiethoff P, Ehrke H-U, Menzel D and Feulner P 1995 *Phys. Rev. Lett.* **74** 3792
- [53] Kassühlke B and Feulner P 2012 *Low Temp. Phys.* **38** 749–54
- [54] Haensel R, Keitel G, Kunz C and Schreiber P 1970 *Phys. Rev. Lett.* **25** 208